Supplemental Material:

Sara J. Fraser-Miller[1], Jeremy S. Rooney[1], Keith C. Gordon[1], Craig R. Bunt[2], Jill M. Haley[3,*]

[1]Department of Chemistry, University of Otago, PO Box 56, Dunedin 9054, New Zealand
[2]Department of Agricultural Sciences, Lincoln University, PO Box 85084, Lincoln 7647, New Zealand
[3]Canterbury Museum, Rolleston Avenue, Christchurch 8013, New Zealand
[*]Corresponding author, JHaley@canterburymuseum.com

Contents

PCA - Raman data

Principle component analysis (PCA) was employed to compare the partial dog cake spectra to model dog cakes (M1 to M4) and a commercially available dog biscuit (Tux) to help identify its contents. The first two principle components (PCs) describe 68 % of the overall spectral variance. In the scores plot (Fig. S1 (a)) each spectrum is represented by a single point, samples with similar spectral signatures will cluster close together and samples with distinct spectra will cluster far apart. This gives a visual guide to how similar or different spectra are to one another and the associated loadings plots give insight into the spectral features leading to separation in scores space.

PC1 separates the bone fragments (positive PC1) from the bulk cakes (negative PC1). Inspection of the associated loadings (Fig. S1 (c)) shows that PC1 separates typical bone signal (961, 1068, 1443 and 1669 cm^{-1}) (Morris & Mandair, 2011; Penel et al., 1998; Thomas et al., 2007) from wheat flour signal (480, 866, 1127, 1337 and 1383 cm^{-1}) (Kizil et al., 2002). The second PC separates the modern model samples (positive PC2) from the partial dog cake samples (negative PC2). The associated loadings (Fig. S1 (c)) appear to separate wheat flour and bone features observed in the dog cakes (positive PC2) from baseline curvature and echeloning artefacts associated with the emissive nature of some samples that was not fully removed during the baseline correction.

The third and fourth PCs yield insight into a further 23 % of spectral variance (Fig. S1 (b)). These PCs provide description of spectral variance more associated with the meat, bone and shortening based spectral differences with the bulk portion of the partial dog cake and model cakes sitting in neutral PC3 and PC4 space. PC3 describes spectral variance between shortening (positive) and bioapatite (negative) based spectral features (Fig. S1(c)). Whilst the fourth PC describes differences in signal between shortening and bone signals (positive PC4) from the meat (negative PC4), Fig. S1 (b) and (c).

These data suggests the presence of bone fragments within the dog cake and a composition more similar to the commercial Tux biscuits than the model dog cakes. However, PC2 is a relatively large source of separation (23 % explained variance) and is heavily influenced by the emissive nature of the samples which make interpretation less clear. Infrared spectroscopy was also carried out to obtain complementary information that was less sensitive to the emissive signal.

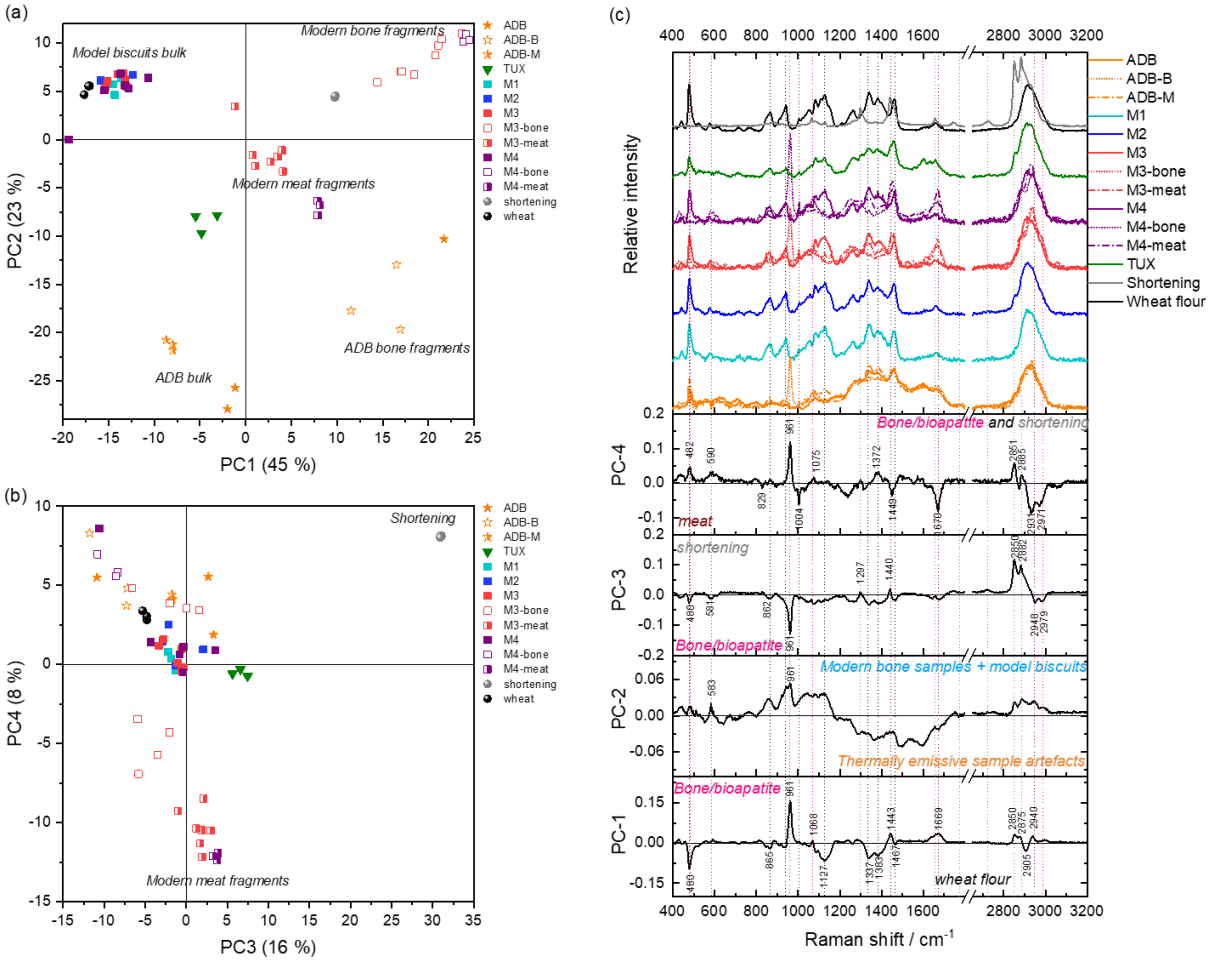

Fig. S1. PCA from FT-Raman spectra collected from the partial dog cake along with model and modern day dog biscuits. (a) Scores plot for PC1 versus PC2, (b) scores plot for PC3 versus PC4, and (c) the associated loadings and comparative spectra.

PCA – FTIR data

The spectra from the partial dog cake were compared using PCA to model dog cakes, a commercial Tux biscuit and reference flour and grains (Fig. S2). The resulting analysis primarily described sources of variation between starches/bulk partial dog cake matrix and shortening based spectral features. More specifically positive PC1 loadings at 1076, 1043, 1016 and 1099 cm^{-1} are associated with polysaccharides (Kizil et al., 2002; Wiercigroch et al., 2017) and negative loadings at 1742 (C=O ester stretching), 1466 (CH_2, CH_3 bending), 1173 (CH_2 stretching, C-O bending) and 723 cm^{-1} (CH_2 and HC=CH bending) are associated

with shortening (Guillen & Cabo, 1997). The differences between meat and shortening/bone (Boskey & Camacho, 2007; Rey, Collins, Goehl, Dickson, & Glimcher, 1989; Yang, Irudayaraj, & Paradkar, 2005) based spectral features are described by PC2 and differences between meat (Hu, Zou, Huang, & Lu, 2017) and bone based spectral features are described by PC3. As all the partial dog cake spectra cluster tightly amongst the model dog cakes and flour samples the PCA was repeated with the shortening, meat and bone based spectra excluded to better explore the variance in the bulk matrix of the partial dog cake and model dog cakes.

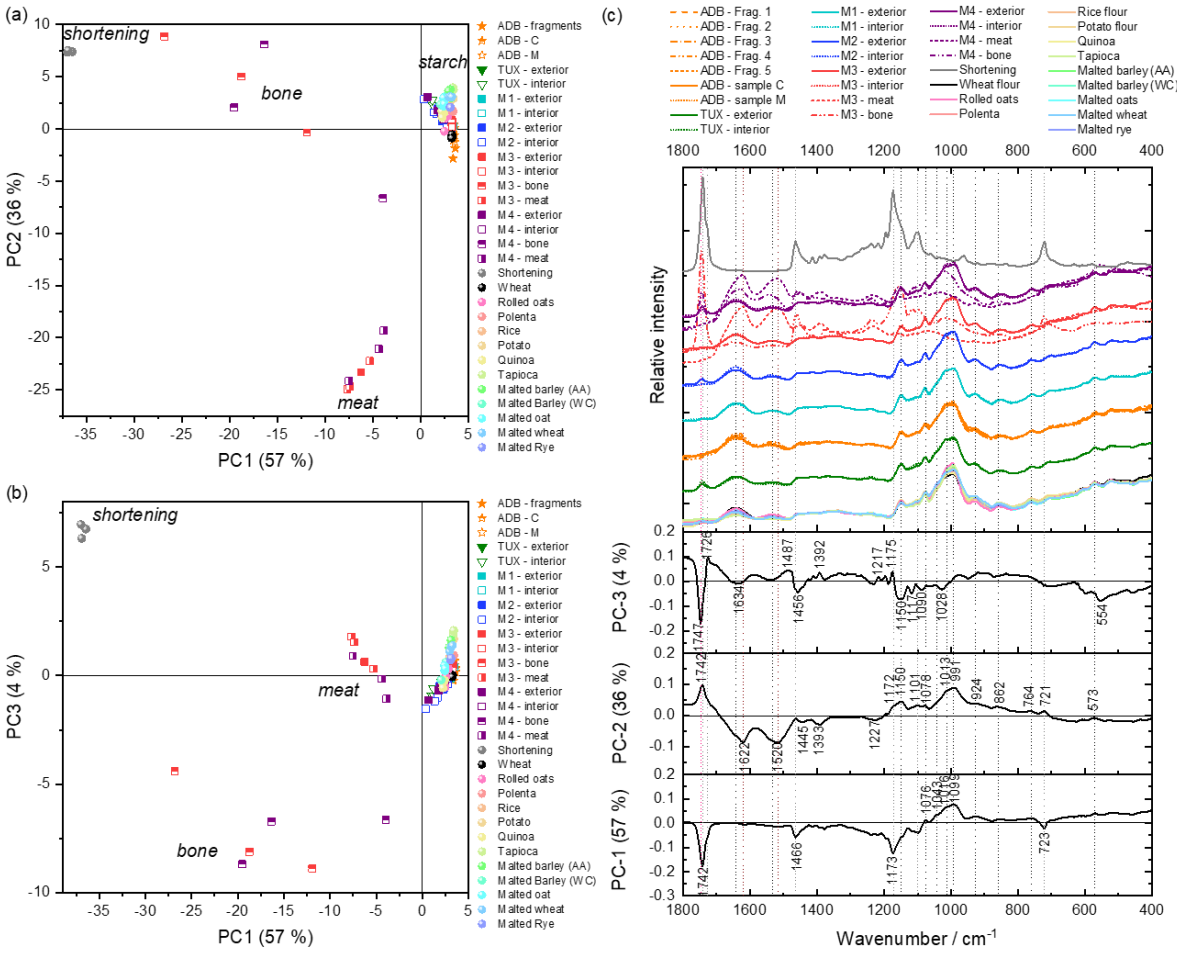

Fig. S2. PCA from FTIR spectra collected from the fragments of the Antarctic dog cake along with model and modern day dog biscuits and reference flours/grains. (a) Scores plot for PC1 versus PC2, (b) scores plot for PC1 versus PC3, and (c) the associated loadings and comparative spectra.

PCA was repeated using the spectra collected only from the bulk matrix of each sample and the reference flours and grains to try gain further insight into the differences between the historical, model and modern day dog biscuits. Some grains and flours included in this analysis, such as quinoa and tapioca, are not expected to have been readily available in England at the time the partial dog cake was made. However they were included to capture the possible variation in different flours and starches. The resulting scores plots (Fig. S3 (a)

and (b)) showed trends along PC1 with the majority of the reference flours and grains sitting in positive PC1 scores space whereas the partial dog cake clustered in negative PC1 scores space alongside wheat flour and rolled oats. The model dog cakes and commercial dog biscuits remained fairly neutral in PC 1 scores space. Separation along PC1 is attributed to the relative abundance of carbohydrate (Wiercigroch et al., 2017) content to protein (Kong & Yu, 2007) content (Fig. S3 (c)).

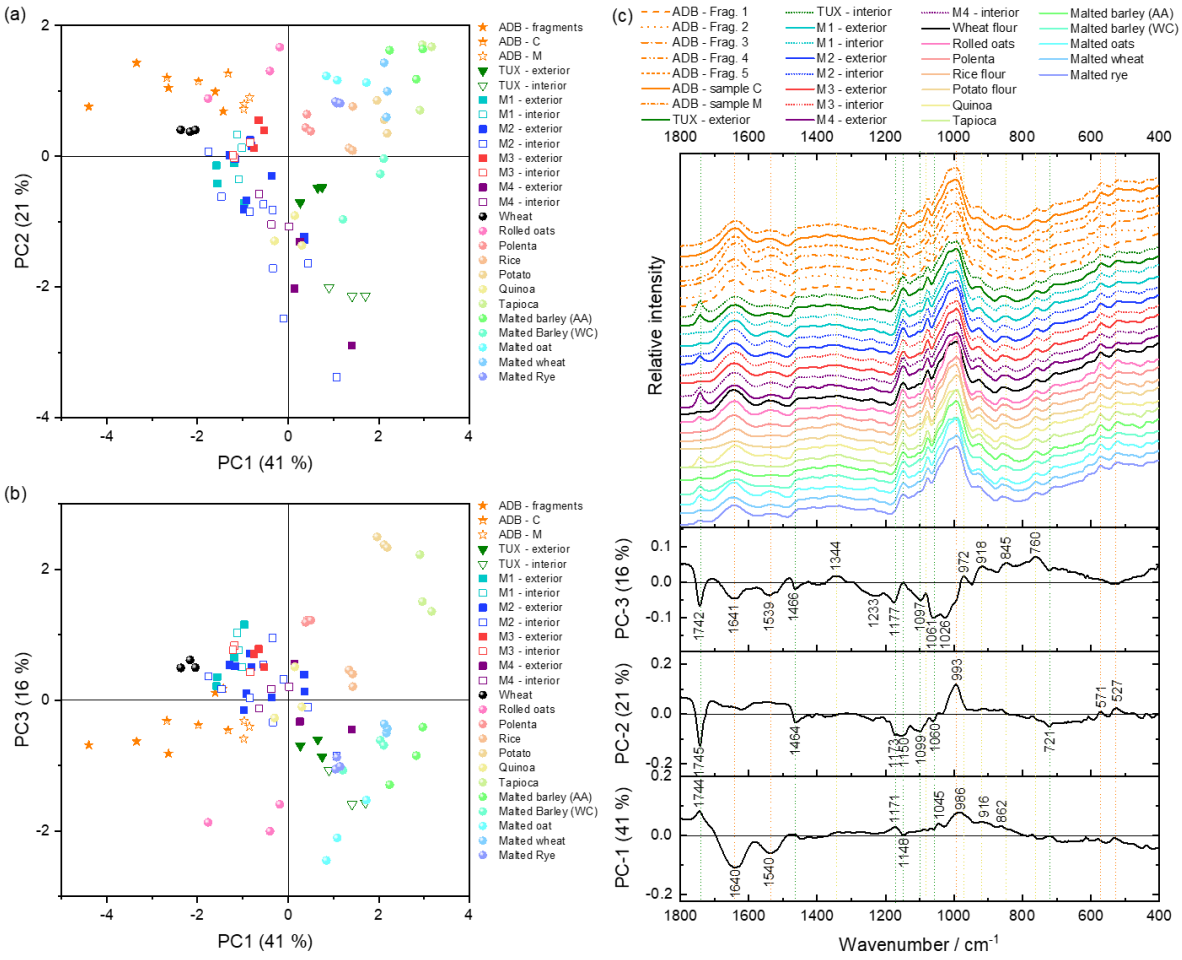

Fig. S3. PCA of the FTIR spectra collected from partial dog cake samples, model and commercial dog cakes and a set of different flours and starches. (a) PC1 versus PC2 scores, (b) PC1 versus PC3 scores and (c) the associated loadings and exemplar spectra.

The second PC separates the partial dog cake and the majority of reference flours and grains from the model dog cakes containing shortening (M2 and M4), the Tux dog biscuit and quinoa (Fig. S3 (a)). The model dog cakes without shortening remained in neutral PC 2 space. The separation is described by the positive features at 993, 571 and 527 cm^{-1} which are attributed to polysaccharides such as amylose and amylopectin in origin (Wiercigroch et al., 2017). These polysaccharides make up the two major components in the starch portion of wheat flour, with starch contributing to 65-70 % of the overall composition (D'Appolonia & Rayas-Duarte, 1994). The negative PC2 loadings features observed at 1745, 1464,

1173/1150, 1099 and 721 cm^{-1} and are attributed to a lipidic origin (fats and oils) (Guillen & Cabo, 1997).

The third PC is separating potato and tapioca flour (positive PC3) from rolled and malted oats (negative PC3). Less separation is observed with the model dog cakes towards positive PC3 space and the Tux dog biscuit and partial dog cake into negative PC3 space. The stated ingredients for the commercially obtained Tux dog biscuit are: Cereals and/or cereal by-products, meat and animal by-products and fats derived from beef and/or sheep and/or poultry and/or goat and/or venison, natural flavour and/or vegetable oil, salt, vitamins and minerals. This differs from the model dog cakes by the following parameters: Salt, possible cereal and meat product type, vitamins and minerals. Salt will not be detected in this analysis as it is used as IR windows and does not absorb light in the spectral window measured ("Sodium Chloride (NaCl)," 2020).

Inspection of the loadings shows that the strongest separating features are associated with minor variation in the shape and position of the peaks predominantly observed in the flour samples. Higher relative signals (that may be attributed to lipid or protein) are observed in negative PC3 space whereas differences in the carbohydrate spectral features are associated with negative and positive PC3 space (Fig. S3 (c)). The Tux dog biscuits are clustering amongst the malted grain signals in PC1 versus PC3 scores space indicating malted oats, barley or rye could be potential cereals used in this biscuit. In all three PCs the partial dog cake samples cluster nearest the wheat flour and rolled oat samples (although not intermingled), the position of the partial dog cake samples in PC space is consistent with partial dog cake containing a mixture of these two cereal sources.

Determination of carbon, hydrogen, nitrogen and sulphur and micro-calorific analysis

The elemental analysis of the carbon, hydrogen and nitrogen percent content of the particles of the partial dog cake designated matrix, bone and meat (Table 1) are consistent with those reported for food waste (49.5, 6.3, 2.9 respectively carbon, hydrogen and nitrogen (Zhang et al., 2013)) and meat and bone (42.8, 5.8, 8.9 respectively carbon, hydrogen and nitrogen (Chaala & Roy, 2003)). It is not surprising the carbon content of particles from the partial dog cake thought to be bone have a much lower carbon content of 19 % compared to the other particles of 39.7 and 38.6 % for matrix and meat respectively, as bone has significant calcium and therefore skews the proportion of carbon to a low content.

Table 1. Summary of the elemental analysis and heating values. Results are the average of duplicates to ≤0.30%.

Sample	Carbon (%)	Hydrogen (%)	Nitrogen (%)	Sulphur (%)	Gross heating value (kJ/kg)	Net heating value (KJ/kg)
Matrix	39.7	6.2	2.4	<0.30	22561	21227
Bone	19.0	3.1	4.3	<0.30	10900	10245
Meat	38.6	5.9	2.9	<0.30	21734	20467

References

Atkins, C., Buckley, K., Blades, M., & Turner, R. (2017). Raman Spectroscopy of Blood and Blood Components. *Applied Spectroscopy, 71*(5), 767-793.

Boskey, A., & Camacho, N. (2007). FT-IR imaging of native and tissue-engineered bone and cartilage. *Biomaterials, 28*(15), 2465-2478.

Chaala, A., & Roy, C. (2003). Recycling of Meat and Bone Meal Animal Feed by Vacuum Pyrolysis. *Environmental Science & Technology, 37*(19), 4517-4522. doi:10.1021/es026346m

D'Appolonia, B., & Rayas-Duarte, P. (1994). Wheat carbohydrates: structure and functionality. In W. Bushuk & V. F. Rasper (Eds.), *Wheat: Production, Properties and Quality* (pp. 107-127). Boston, MA: Springer US.

de Oliveira, V., Castro, H., Edwards, H., & de Oliveira, L. (2010). Carotenes and carotenoids in natural biological samples: a Raman spectroscopic analysis. *Journal of Raman Spectroscopy, 41*(6), 642-650.

Doblado-Maldonado, A., Pike, O., Sweley, J., & Rose, D. (2012). Key issues and challenges in whole wheat flour milling and storage. *Journal of cereal science, 56*(2), 119-126.

Gerth, N., Redman, P., Speakman, J., Jackson, S., & Starck, J. (2010). Energy metabolism of Inuit sled dogs. *Journal of Comparative Physiology B, 180*(4), 577-589.

Guillen, M., & Cabo, N. (1997). Infrared spectroscopy in the study of edible oils and fats. *Journal of the Science of Food and Agriculture, 75*(1), 1-11.

Hervera, M., Castrillo, C., Albanell, E., & Baucells, M. (2012). Use of near-infrared spectroscopy to predict energy content of commercial dog food. *Journal of animal science, 90*(12), 4401-4407.

Hinchcliff, K., Reinhart, G., Burr, J., Schreier, C., & Swenson, R. (1997). Metabolizable energy intake and sustained energy expenditure of Alaskan sled dogs during heavy exertion in the cold. *American journal of veterinary research, 58*(12), 1457-1462.

Hu, Y., Zou, L., Huang, X., & Lu, X. (2017). Detection and quantification of offal content in ground beef meat using vibrational spectroscopic-based chemometric analysis. *Scientific reports, 7*(1), 15162.

Kizil, R., Irudayaraj, J., & Seetharaman, K. (2002). Characterization of irradiated starches by using FT-Raman and FTIR spectroscopy. *Journal of agricultural and food chemistry, 50*(14), 3912-3918.

Kong, J, & Yu, S. (2007). Fourier transform infrared spectroscopic analysis of protein secondary structures. *Acta biochimica et biophysica Sinica, 39*(8), 549-559.

Morris, M., & Mandair, G. (2011). Raman Assessment of Bone Quality. *Clinical Orthopaedics and Related Research, 469*(8), 2160-2169.

Ozaki, Y., Mizuno, A., Sato, H., Kawauchi, K., & Muraishi, S. (1992). Biomedical application of near-infrared Fourier transform Raman spectroscopy. Part I: the 1064-nm excited Raman spectra of blood and met hemoglobin. *Applied Spectroscopy, 46*(3), 533-536.

Penel, G., Leroy, G., Rey, C., & Bres, E. (1998). MicroRaman spectral study of the PO_4 and CO_3 vibrational modes in synthetic and biological apatites. *Calcified Tissue International, 63*(6), 475-481.

Rey, C., Collins, B., Goehl, T., Dickson, I., & Glimcher, M. (1989). The carbonate environment in bone mineral: a resolution-enhanced Fourier transform infrared spectroscopy study. *Calcified Tissue International, 45*(3), 157-164.

Sodium Chloride (NaCl). (2020). Retrieved from https://www.crystran.co.uk/optical-materials/sodium-chloride-nacl

Thomas, D., Fordyce, R., Frew, R., & Gordon, K. (2007). A rapid, non-destructive method of detecting diagenetic alteration in fossil bone using Raman spectroscopy. *Journal of Raman Spectroscopy, 38*(12), 1533-1537.

USDA National Nutrient Database for Standard Reference, Release 28 (Slightly revised). Version Current: May 2016. . (2016). Retrieved from http://www.ars.usda.gov/nea/bhnrc/mafcl

Uysal, R., Boyaci, I., Genis, H., & Tamer, U. (2013). Determination of butter adulteration with margarine using Raman spectroscopy. *Food Chemistry, 141*(4), 4397-4403.

Weiss, W., & Tebbe, A. (2018). Estimating digestible energy values of feeds and diets and integrating those values into net energy systems. *Translational Animal Science, 3*(3), 953-961. doi:10.1093/tas/txy119

Wiercigroch, E., Szafraniec, E., Czamara, K., Pacia, M., Majzner, K., Kochan, K., . . . Malek, K. (2017). Raman and infrared spectroscopy of carbohydrates: A review. *Spectrochimica Acta Part A: Molecular and Biomolecular Spectroscopy, 185*, 317-335.

Yang, H., Irudayaraj, J., & Paradkar, M. (2005). Discriminant analysis of edible oils and fats by FTIR, FT-NIR and FT-Raman spectroscopy. *Food Chemistry, 93*(1), 25-32.

Zhang, Y., Arnold, R., Paavola, T., Vaz, F., Neiva Correia, C., Cavinato, C., . . . Heaven, S. (2013). Compositional analysis of food waste entering the source segregation stream in four European regions and implications for valorisation via anaerobic digestion.